Single-Stage Boost Inverter with Coupled Inductor fed PMBLDC Motor

SAMBASIVA RAO YALALA [1], J.RAMA CHANDRA RAO[2],
[1]Department of EEE, Swarnandra College of Engineering and Technology, Narsapuram- 534 280
[2]Department of EEE, Swarnandra College of Engineering of Technology, Narsapuram- 534 280
[1]**Email:** ysambaa@gmail.com ,[2]**Email:** jrr_chandra@yahoo.com .

***Abstract*—This paper proposes a single-stage boost-type inverter by introducing impedance network, including coupled Inductor, into the three-phase bridge inverter. By adjusting the forbidden shoot-through zero state, the converter can realize a high boost gain and a stable ac output voltage. The single-stage operation of the converter may lead to improved reliability and higher efficiency. For distributed generation units of Renewable power systems experience big changes in the inverter input voltage due to fluctuations of energy resources. A front-end boost converter is added to step up the dc voltage when the energy resources are at a weak point. However, when a very high boost gain is demanded, the duty cycle may come to its extreme and large duty cycles causes serious reverse-recovery problems. finally the PMBLDC Motor is implemented through a three-phase VSI fed from a controlled DC link voltage (or)Bus Voltage for suitable applications. Also the HALL SENSORS are used at PMBLDCM to feed back to the VSI. Therefore the VSI is operated only as an electronic commutation of the PMBLDCM and speed control of PMBLDC Motor is open loop control.**

***Index Terms*—Boost inverter, coupled inductor, Permanent Magnet Brushless DC Motor, shoot-through zero state, single stage.**

I. INTRODUCTION

THE increasing tension on the global energy supply has resulted in greater interest in renewable energy resources [1].This presents a significant opportunity for distributed power generation (DG) systems using renewable energy resources, including wind turbines, photovoltaic (PV) generators, small hydro systems, and fuel cells [2]–[4]. However, these DG units produce a wide range of voltages due to the fluctuation of energy resources and impose stringent requirements for the inverter topologies and controls [5]. Usually, a boost-type dc–dc converter is added in the DG units to step up the dc voltage [6]–[8].This kind of topology, although simple may not be able to provide enough dc voltage gain when the input is very low, even with an extreme duty cycle. Also, large duty cycle operation may result in serious reverse-recovery problems and increase the ratings of switching devices. Furthermore, the added converter may deteriorate system efficiency and increase system size, weight, and cost. On the other hand, the upper and lower devices of the same phase leg cannot be gated on simultaneously in conventional voltage source inverter (VSI). Otherwise, shoot Through problems would occur and destroy the switching devices. Dead time is always used in case of shoot-through Events in bridge type converters, but it will cause waveform distortion. Though dead-time compensation technology [9], [10] has been developed, it increases control complexity. So, it is desirable to have a single-stage high-gain boost inverter featuring no shoot through issues.

Single-stage topologies, which integrate performance of each stage in a multistage power converter, are becoming the focus of research. Though they may cause increased control Complexity, they may offer higher efficiency, reliability, and lower cost. It is observed that many single-stage voltage source [11]–[13] and current source [14], [15] inverters have been proposed. A Z-source inverter (ZSI) proposed in [16] is able to overcome the problems in conventional VSI and conventional current source inverter. It can provide a wide range of obtainable voltage and has been applied to renewable power generation systems [17]–[19]. However, this topology is complex and inductors and capacitors in the Z-network should have high consistency. Moreover, only shoot-through zero state can be regulated when higher voltage gain is required. Widening shoot-through zero state will decrease modulation index and output voltage amplitude. Also, in order to completely avoid the unwanted operation modes, the input diode should be replaced by a switch which turns ON during all active states and traditional zero states [20]. Four quasi-Z-source inverters (qZSIs) derived from the conventional ZSI have been proposed in [21], whose basic principles are similar to those of conventional ZSI. Corresponding control methods and application conditions of conventional ZSI also fit for the qZSIs in theory. Anderson and Peng [21] show some advantages of qZSIs over conventional ZSI, such as lower voltage/current stress of impedance network and lower switch voltage stress. Nevertheless, they do not overcome the limits of conventional ZSI described earlier.

This paper presents a novel single-stage boost inverter with a unique impedance network including coupled inductor. The bus voltage can be stepped up by using shoot-through zero state to store and transfer energy within the impedance network. Just as with ZSI, the single-stage boost inverter completely avoids destroying devices during shoot-through zero states. So, it has improved reliability. Second, the inductors and capacitors do not have to be of consistency, leading to easier circuit parameters design. Third, both shoot-through zero states and coupled inductor's turn ratio can be regulated to control the boost gain So, the output voltage can be regulated in a wide range and can be stepped up to a higher value. Finally, the bus voltage equals the sum of the capacitor voltages, and it is higher than each capacitor voltage. This

ensures status capacitor voltage ratings can be fully utilized. The single-stage boost inverter with coupled inductor is suitable for applications where the input voltage varies from a relative low level to a higher level continuously while outputting a stable ac voltage. Operating principles of the novel inverter are presented in Section II. Section III analyzes the equivalent circuit, boost feature under two different modes, and its control strategy. In Section IV, the coupled inductor is analyzed. Finally, simulation and experiment results are included in Section V. analyzed. Finally, simulation and experiment results are included in Section V.

II. PROPOSED SINGLE-STAGE BOOST INVERTER WITH PMBLDC MOTOR

Fig. 1 shows the general structure of the proposed single stage boost inverter. It employs a unique impedance network to combine the three-phase inverter bridge with the power source. The impedance network does not introduce any switching devices and may lead to improved reliability, higher efficiency, and lower cost. To extend the operation range of the inverter, coupled inductor with a low leakage inductance is used. The dc source can be a battery, diode rectifier, fuel cell, or PV cell. To describe the operating principle and characteristics, this paper focuses on one application example of the single-stage boost inverter:a single-stage boost inverter for wind power generation.

For wind power generation system, variable speed wind turbine is often adopted because it is known to provide more effective power tracking than fixed speed wind turbines [22]. Fig. 2 presents the relationship between the generator power output and rotational speed relating to wind speed changes. Note that the output power of wind turbine may be at a low level under a weak wind condition. Fig. 3 shows the conventional twostage power conversion for wind power generation. A front-end dc–dc boost converter is added to step up bus voltage especially under weak wind condition, because the conventional VSI cannot produce an ac voltage larger than the dc input voltage. The proposed single-stage boost inverter for wind power generation application is shown in Fig. 4. The system can produce an ac voltage larger or smaller than the input dc voltage with single stage operation. The diode D1 in series with Lp is necessary for preventing reverse current flow.

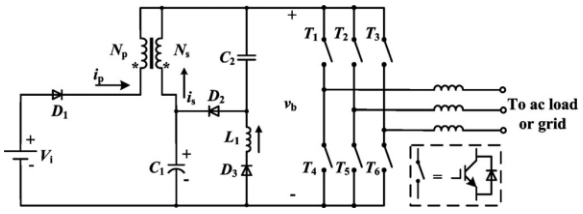

Fig. 1. Topology of single-stage boost inverter with coupled inductor

The proposed PMBLDC Motor scheme shown in fig4.2 controls reference voltage at DC link as an equivalent reference speed, thereby replaces the conventional control of the motor speed and a stator current involving various sensors for voltage and current signals. Moreover, the rotor position signals are used to generate the switching sequence for the VSI as an electronic

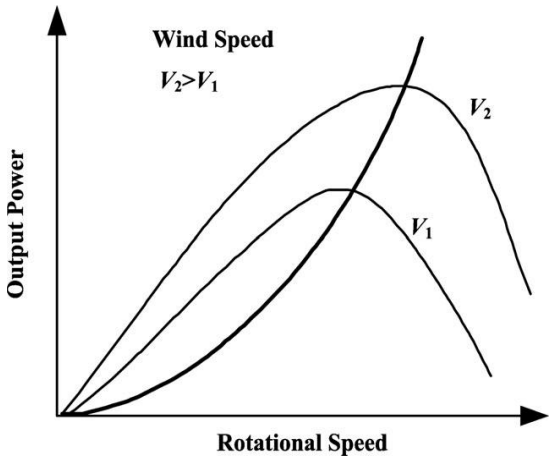

Fig. 2. Relationship between the generator output power

And rotational speed.

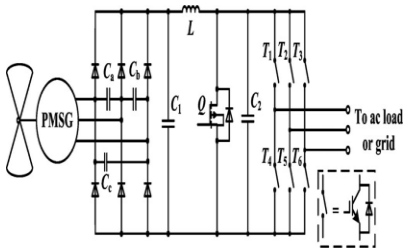

Fig.3. Traditional two-stage power conversion for wind power generation.

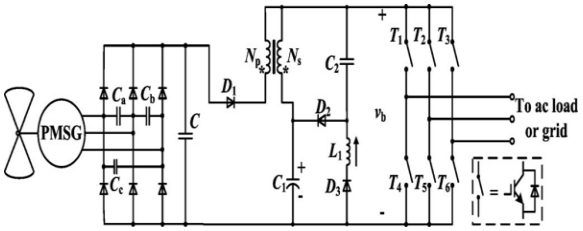

Fig. 4.1.Single stage boost inverter with coupled inductor for wind power generation.

Moreover, the rotor position signals are used to generate the switching sequence for the VSI as an electronic commutation of the PMBLDC motor. Therefore, rotor-

position information is required only at the commutation points, e.g., every 60°electrical in the three- phase [1-4]. The rotor position of PMBLDCM is sensed using Hall Effect position sensors and used to generate switching sequence for the VSI. In this trapezoidal back emf PMBLDCM is used.

The DC link voltage is controlled by a boost DC-DC converter based on the duty ratio (D) of the converter. For a fast and effective control with reduced size of magnetics and filters, a high switching frequency is used; however, the switching frequency (f_S) is limited by the switching device used, operating power level and switching losses of the device. Metal oxide field effect transistors (MOSFETs) are used as the switching device for high switching frequency in the proposed PFC converter. However, insulated gate bipolar transistors (IGBTs) are used in VSI bridge feeding PMBLDCM, to reduce the switching stress, as it operates at lower frequency compared to PFC switches.

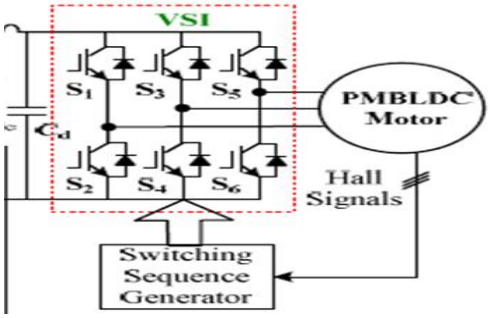

(a)

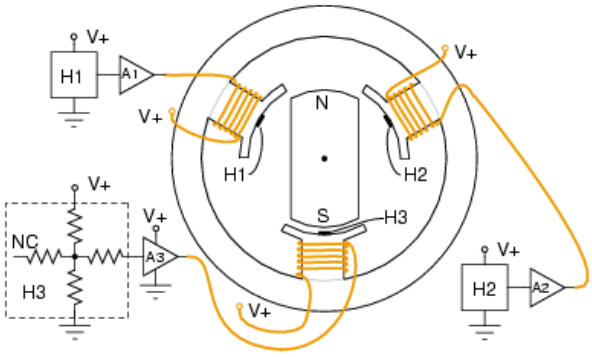

(b)

Fig 4.2.(a)VSI fed to the PMBLDCM (b)PMBLDC with HALL SENSORS

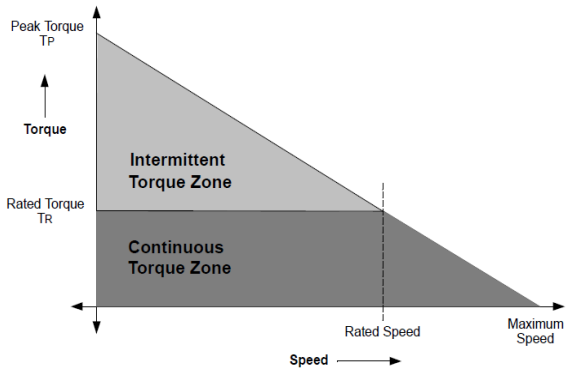

Fig.4.3.Speed torque characteristics of the PMBLDC

The speed torque characteristics shown in fig.4.3.torque remains constant at rated speed after the rated speed the torque will be dropped. So the ratings of the motor fixed as per the speed torque characteristics. In this motor will be controlled in open loop so the motor is used for constant speed applications

III. OPERATION PRINCIPLE, BOOST FEATURE ANALYSIS AND CONTROL STRATEGY

Conventional VSI has eight possible switching states [23], of which two are zero states and six are active states. Two zero states make load terminals shorted through, and can be assumed by turning on upper or lower three devices, respectively. Six active states can be assumed by turning on the switches from different phase legs, when the input dc voltage is applied across the load. However, the three-phase single-stage boost inverter has one extra zero state when the load terminals are shorted through both the upper and lower devices of any one phase leg, any two phase legs, or all three phase legs. To distinguish the two kinds of zero state mentioned earlier, we call the two zero states open-zero states, and the extra zero states shoot through zero state. Shoot-through zero state is forbidden in the conventional VSI because it would make device failure events happen. Combined with the impedance network in front of the three-phase bridge, the shoot-through zero state provides the unique boost feature to the inverter. It should be noted that shoot-through zero states are allocated into open-zero states without changing the total open-zero state time intervals. That is, the active states are unchanged. Thus, the shoot-through zero state does not affect the pulse width modulation (PWM) control of the inverter, because it equivalently produces the same zero voltage as the open-zero state to the load terminal. Fig. 5 shows equivalent circuits of the single-stage boost inverter under three switching states.

State 1: The converter is in shoot-through zero state under this duration, as shown in Fig. 5(a). Bus voltage *vb* was shorted to ground and diode *D*2 is reversely biased. Input dc voltage is applied across primary winding of the coupled inductor, making primary current linearly increase. The inductive voltage of secondary winding charges *C*1. At the

same time, *C*2 is discharged by *L*1 with linearly increasing current, assuming that the capacitor voltage is constant.

State 2: During this interval, the converter is in one of the two traditional open-zero states, as shown in Fig. 5(b). Inductor *L*1and secondary winding of the coupled inductor charge capacitors *C*1 and *C*2 through diode *D*2 , respectively. In this state, the current of inductor *L*1 decreases from peak value to zero.

State 3: When the circuit is in one of the six active states, as shown in Fig. 5(c), diode *D*3 is reverse biased. The energy stored in the coupled inductor and *C*1 releases to the load, and the bus voltage is stepped up to a higher level.

Two boost modes can be achieved by regulating the shoot through zero state as well as configuring the turn ratio and coupling coefficient of the coupled inductor. Operating principle of the single-stage boost inverter is analyzed under these two modes. When applying the converter to voltage drop compensation or applications where lower boost gain is needed, the inductance of coupled inductor should be designed large enough to ensure its continuous current-mode operation. When higher boost gain is required, the inductance of the primary winding *Lp* should be as small as to keep the circuit working in discontinuous current mode. Fig. 6 shows coupled inductor current waveform in one shoot-through period *T*sh under two operation modes, respectively. Note that the shoot-through period *T*sh is the equivalent switching period viewed from the impedance network, which is not equivalent to the switching period *Ts* of the inverter bridge. *T*sh may be two or six times of *Ts* , determined by the modulation scheme it used [16], [24], [25], which reduces the required size and weight of the coupled inductor.

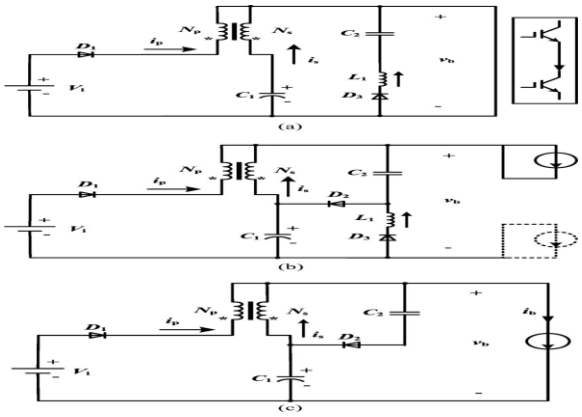

Fig. 5. Equivalent circuit under three switching states. (a) Shoot-through zero state. (b) Open-zero state. (c) Active state.

A. Lower Voltage Boost Gain Mode

In lower voltage boost gain applications, the key characteristic is that the current through *Lp* generally works in continuous mode, as shown in Fig. 6(a).

Define the shoot-through duty cycle *D*0 as the time when the three-phase bridge is in shoot-through state, and the duty cycle 1 − *D*0 as the time when the three-phase bridge is in non shoot through state, the average voltage across the primary winding during one shoot-through period can be expressed

$$(v_{Lp}(t))_{Tsh}^{CCM} = D_0 Vi + (1-D0)(Vi-vb) = 0 \qquad (1)$$

From (1), the amplitude of bus voltage can be expressed as follows:

$$\widehat{v_b} = \frac{1}{1-D_o} \times V_i \qquad (2)$$

Define *B* as the boost gain,$B=v_bV_i$ can be expressed as

$$B=\frac{1}{(1-Do)} \qquad (3)$$

The boost gain is similar to that of conventional dc-dc boost converter in this boost mode.

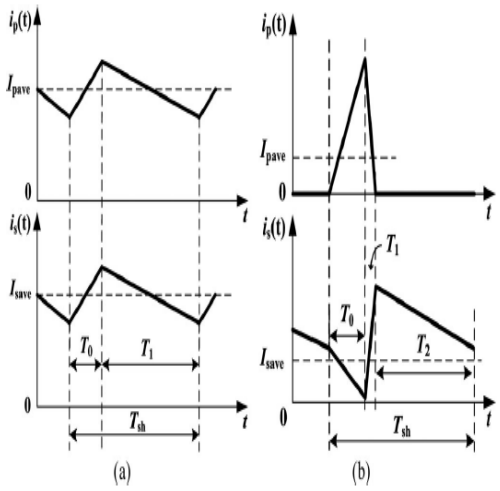

Fig. 6. Coupled inductor current waveforms under two operation modes. (a) Inductor *Lp* works in CCM. (b) Inductor *Lp* works in DCM.

B. Higher Voltage Boost Gain Mode

In higher voltage boost gain applications, the key characteristic is that the inductance of primary winding is less

than that of secondary winding, and primary winding current generally works in discontinuous mode, as shown in Fig. 6(b).

Define the coupling coefficient as

$$k=\frac{M}{\sqrt{Lp+LS}} \qquad (4)$$

where *Lp* , *Ls* , and *M* are the self-inductance of each winding and the mutual inductance, and the effective turn ratio

$$N_e=\sqrt{\frac{L_s}{L_p}} \qquad (5)$$

Define the duty cycle *D*1 as the time when the inductor *Lp* current decreasing from peak value to zero, the average voltage across the both sides of coupled ind inductor during one shoot through period can be expressed as

$$(v_{Lp}(t))_{Tsh}^{DCM}=D_0V_i+D_1(V_i-v_b)+(1-D_0-D_1)$$

$$k\frac{(V_{c1}-v_{b)}}{N_e}=0 \qquad (6)$$

$$(v_{Ls}(t))_{T_{sh}}^{DCM}=D_0V_{c1}+(1-D_0)=0 \quad (7)$$

From (6) and (7), the amplitude of bus voltage can be expressed as

$$\widehat{v_b}=\frac{(D_0+D_1)N_e}{D_1N_e+D_0(1-D_0-D_1)}\times V_i \quad (8)$$

Define physical turn ratio of ideal transformer as *N = Ns /Np* . According to the relationship of *Ne* and *N*: *N= N × k*, (8) can be simplified as

$$B=\frac{\widehat{v_b}}{V_i}=\frac{(D_0+D_1)N}{D_1N+D_0(1-D_0-D_1)} \qquad (9)$$

The output peak phase voltage ˆ*vac* generated by the inverter can be expressed as

$$\widehat{v_{ac}}=mB\frac{V_i}{2} \qquad (10)$$

Where *m* is the modulation index, $m \le 1$ for synchronized PWM(SPWM), and $m \le 2/\sqrt{3}$ for space vector PWM. The output ac voltage can be stepped up or down by choosing an appropriate voltage gain *G*

$$G=m\times B \qquad (11)$$

From (11), the voltage gain *G* is determined by the modulation index *m* and boost gain *B*. The available output ac voltage is able to change in a wide range by regulating *G*. The boost gain *B* as expressed in (9) can be controlled by shoot-through duty cycle *D*0 , duty cycle *D*1 , and physical turn ratio *N* of the coupled inductor. It should be noted that the available shoot-through duty cycle is limited by the traditional open-zero duty cycle which is determined by the modulation index *m*. The shoot-through zero state does not affect the PWM control of the inverter, because it equivalently produces the same voltage to the load terminal.

As analyzed earlier, by designing different coupled inductor and regulating the duty cycle, the single-stage boost inverter not only can be applied to voltage drop compensation or applications where lower boost gain is needed, but it can also can be applied to higher boost requirements.

The capacitor *C*1 and *C*2 voltage are dependent on the shoot through state and can be stepped up by changing the shoot through duty cycle. The average bus voltage is identical to the capacitor *C*1 voltage because the average voltage across secondary winding of coupled inductor during one shoot-through period is zero.

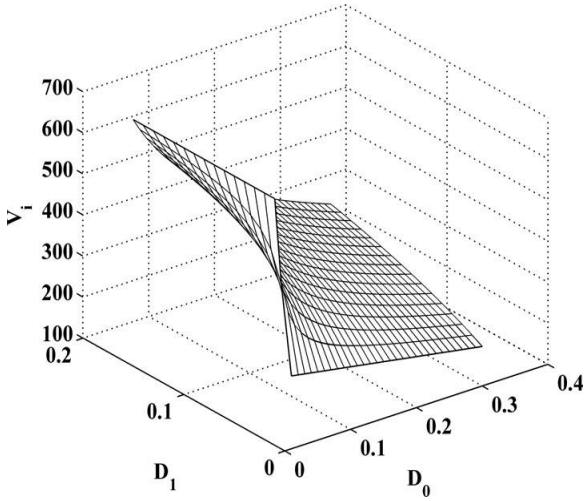

Fig. 7. Relation curve of duty cycle *D*0 , *D*1 , and input voltage *Vi* .

The capacitor *C*1 and *C*2 voltage can be expressed as

$$V_{c1}=\widehat{v_b}\times(1-D_0) \quad (12)$$

$$V_{C2}=\hat{v}_b\times D_0) \qquad (13)$$

When the voltage at the diode bridge output provided by the generator in wind power generation system is approximately

300 Vdc, without any boost mode, the voltage at the inverter bridge input will also be approximately 300 Vdc. The inverter can only output a phase voltage of 106 Vrms based on SPWM control under modulation index *m* being 1. In order to obtain phase voltage of 220 Vrms , the minimum voltage at the inverter bridge input must be greater than 620Vdc. Therefore, the voltage at the diode bridge output needs to be boosted, and the single stage boost inverter with higher boost gain should be used. According to aforementioned analysis, in higher voltage boost gain applications, boost gain *B* as expressed in (9) is not only determined by shoot-through duty cycle *D*0 , but also by duty cycle *D*1 , and the physical turn ratio of coupled inductor. Duty cycle *D*1 can be expressed as

$$D_1 = \frac{[(NV_i - (1-D_0)\hat{v}_b)]D_0}{(N-D_0)v_b - NV_i} \qquad (14)$$

From (14), we know that when physical turn ratio *N* is determined, duty cycle *D*1 varies with shoot through duty cycle *D*0 , input voltage *Vi* , and bus voltage *vb* .Bus voltage amplitude of the converter is regulated by closed-loop control of shoot-through duty cycle, so *D*1 only varies with input voltage *Vi* when bus voltage amplitude is preset. Fig. graphically illustrates the relationship between shoot-through duty cycle *D*0 , duty cycle *D*1 , and input voltage *Vi* , given a constant physical turn ratio.From Fig. 7, we know that when shoot-through duty cycle *D*0 is determined, duty cycle *D*1 have a certain relationship with input voltage *Vi* .
According to $Ne = N \times k$, (14) can be rewritten as

$$D_1 = \frac{[\frac{N_e}{k} - (1-D_0)B]D_0}{\left(\frac{N_e}{k} - D_0\right)B - N_e/k} \qquad (15)$$

Combined with (5) and (15), we know that when inductances of the coupled inductor are fixed, the effective turn ratio *Ne* is determined. Because bus voltage is regulated by means of closed-loop control of shoot-through zero state, duty cycle *D*1 only varies with coupling coefficient *k* when boost gain is determined .Fig. 8 graphically illustrates the boost gain *B* versus shoot-through duty cycle *D*0 , when inductances of the coupled inductor are fixed. In Fig 8 (a), mode 1, *D*1 = 0, primary winding current decreases from peak value to zero instantly when the coupled inductor is under unity coupling condition. The boost gain of mode 1 is theoretically the maximum gain that the single stage boost inverter can obtain with a given shoot-through zero state: *N*/1-*D*0 . While in Fig. 8 (b), mode 2, *D*1 = 1 − *D*0, primary winding works in continuous current mode. The boost gain is potentially at its minimum value that the single-stage boost inverter can obtain with a given shoot-through zero state: 1/1 − *D*0 .

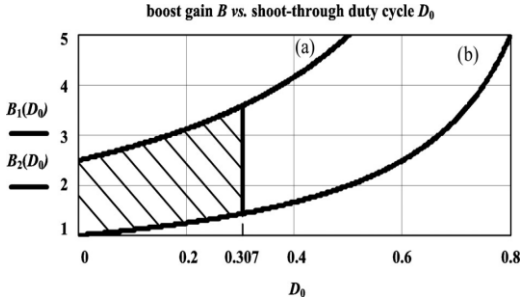

Fig. 8. Boost gain *B* versus shoot-through duty cycle *D*0 .

The previous analysis reveals that 1) with a determined physical turn ratio *N* of the coupled inductor, only shoot-through zero state is required to be regulated to step up and stabilize the bus voltage when input voltage varies in a wide range; and 2) given a constant shoot-through duty cycle *D*0,duty cycle *D*1decreases and boost gain *B* increases as coupling coefficient *k* increases. In other words, when boost gain is determined, duty cycle *D*0 can be decreased to a certain degree by increasing the coupling coefficient *k*, which brings the benefit of reducing primary winding current ripple. All the traditional PWM schemes can be used to control the inverter. Fig. 9 shows the maximum constant boost control method with third-harmonic injection [25]. The equivalent dc bus voltage is boosted because of the shoot-through zero states. Shooting through three phase legs at the same time can reduce the current stress of each device, while the switching frequency is doubled. Meanwhile, the shoot-through states should preferably have the same time duration to minimize the size of the impedance network. When the modulation index *m* is set, the shoot-through duty cycle *D*0 versus modulation index *m* can be expressed as follows:

$$D_0 = 1 - \frac{\sqrt{3m}}{2} \qquad (16)$$

So, the maximum shoot-through duty cycle is limited by modulation index. When the modulation index is set to no less than 0.8, the shoot-through duty cycle is limited to 0.307. The dashed area of Fig. 8 is the possible operation area of the inverter when *N* = 2.5.

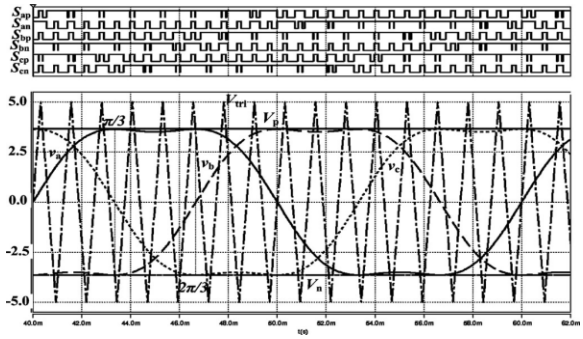

Fig. 9. Maximum constant boost control method with third harmonic injection

IV. COUPLED INDUCTOR DESIGN ANALYSIS

As analyzed earlier, the bus voltage of the proposed converter can be stepped up to a higher level by regulating the shoot-through duty cycle and configuring the turn ratio and the coupling coefficient of the coupled inductor. This paper takes higher voltage boost gain applications as an example to demonstrate the operating principle of coupled inductor in detail.

A. *Transformer Model of Coupled Inductor*

Transformer model can be derived mathematically [26] and can be expressed by the following equations:

$$v_p = L_p \frac{di_p}{dt} + M \frac{di_s}{dt}$$

$$v_s = M \frac{di_p}{dt} + L_s \frac{di_s}{dt} \qquad (17)$$

where mutual inductance *M* is positive under direct coupling condition. The expressions can be rearranged as follows:

$$v_p = L_p \left(1 - \frac{M^2}{L_P L_s}\right) \frac{di_p}{dt} + \frac{M}{L_s} v_s$$

$$v_s = \frac{M}{L_p} v_p + L_s \left(1 - \frac{M^2}{L_p L_S}\right) \frac{di_s}{dt} \quad (18)$$

Assuming that *Lp* = *L*, (4) and (5) can be expressed as

$$L_s = N_e^2 \; L_p = N^2 k^2 L$$

$$M = k\sqrt{L_P} L_s = k^2 N L \quad (19)$$

According to (4) and (19), (18) can be simplified as

$$v_p = L(1 - k^2) \frac{di_p}{dt} + \frac{1}{N} v_s$$

$$v_s = k^2 N v_p + (Nk)^2 (1 - k^{2)} L \frac{di_s}{dt} \quad (20)$$

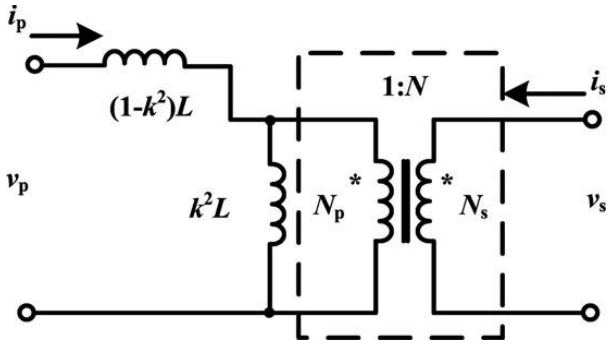

Fig. 10. Equivalent circuit of coupled inductor.

According to (20), an equivalent circuit can be constructed as shown in Fig. 10, where (1 − *k*2)*L* and *k*2 *L* refer to leakage inductance *Lk* and magnetizing inductance *Lm*, respectively. This circuit is one form of the transformer models for coupled inductor, where the leakage inductor appears only on one side.Hence, the coupled inductor is modeled as a magnetizing inductor, an ideal transformer with a turn ratio of *N*, and a leakage inductor.

B. Coupled Inductor Design Guideline

Rewrite (17) as

$$v_p - \frac{k}{N_e} v_s = (1 - K^2) L \frac{di_p}{dt}$$

$$v_s - N_e k v_p = N_e^2 (1 - k^2) L \frac{di_s}{dt} \quad (21)$$

If the relationship of *vp* and *vs* can be found in different time intervals during one shoot-through period *T*sh , (21) can be expressed as

$$v_p = L_{eq\_p} \frac{di_s}{dt}$$

$$v_s = L_{eq-s} \frac{di_s}{dt} \quad (22)$$

Where *L*eq *p* and *L*eq *s* are equivalent inductances of the coupled inductor at different time intervals. It is the same format as the non coupling inductor. The relationship of *vp* and *vs* changes at different time intervals during one shoot-through period. Thus, during different time intervals, the equivalent inductances in (22) are different. As analyzed in Section III, in higher voltage boost gain applications, one shoot-through period *T*sh can be divided into three parts: *T*0 = *D*0*T*sh , *T*1 = *D*1*T*sh , and *T*2 = (1 − *D*0 −*D*1)*T*sh . According to the transformer model constructed earlier,the equivalent inductances can be expressed as

$$L_{eq0\_p} = \frac{1-k^2}{1-(\frac{(1-D_0)(D_0+D_1)}{D_1 N}+D_0(1-D_0-D_{1)}} L$$

T0:

$$L_{eq0_s} = \frac{N^2k^2(1-k^2)}{1-(\frac{D_1N-D_0(D_0+D_1-1)k^2}{(1-D_0)(D_0+D_1)})} L \quad (23)$$

$$L_{eq1\_p} = \frac{1-k^2}{1-\left(\frac{D_0+D_1}{N}\right)-(1-D_0-D_1))} L$$

T1,$L_{eq1\_p} = \frac{N^2k^2(1-K^2)}{1-(\frac{(N-(1-D_0-D_1)k^2)}{D_0+D_1})} L$ (24)

$$L_{eq2\_p} = 0$$

T_2:

$$L_{eq2\_s} = N^2k^2L$$

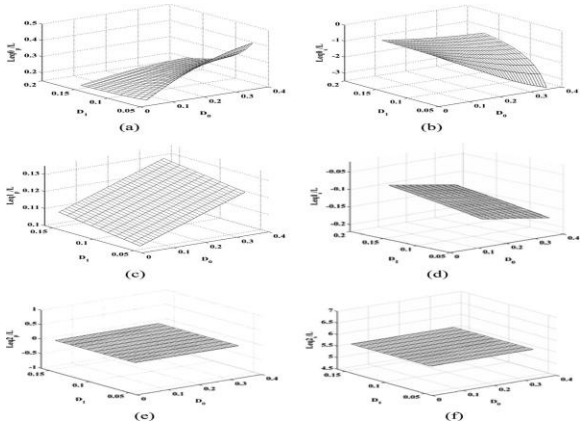

Fig. 11. L_{eqx_p}/L or L_{eqx_s}/L versus duty cycle D_0 and D_1 , (x = 0, 1, 2). (a) L_{eq0_p}/L. (b) L_{eq0_s}/L. (c) L_{eq1_p}/L. (d) $L_{eq1\ s}/L$. (e) $L_{eq2\ \_p}/L$. (f) $L_{eq2\ \_s}/L$.

In higher voltage boost gain applications, primary winding generally works in discontinuous current mode. So, in the active states, L_{eq2_p} is equal to zero because primary winding current is zero. After the bus voltage amplitude and parameters of the coupled inductor are confirmed, the equivalent inductance of different time intervals varies with duty cycle D_0 and D_1 . Fig. 11 graphically illustrates $L_{eqx\ \_p}/L$ or $L_{eqx\ s}/L$ versus duty cycle D_0 and D_1, (x = 0, 1, 2) when N = 2.5 and k = 0.95. In T_0 and T_1 of one shoot-through period T_{sh} ,secondary equivalent inductance versus L: $L_{eq0\ s}/L$ and $L_{eq1\ s}/L$, are negative because secondary winding current is opposite to the reference direction shown inFig.1.Taking the input/output parameters of experimental prototype as an example, according to the equivalent inductance expressions at different time intervals of one shoot-through period T_{sh} and the relationship of inductor voltage and current, which can be expressed as

$$i_{q(n)} = i_{p(n-1)} + \frac{v_p}{L_{eqx\_p}} t \quad \begin{cases} n = 1,2,3 \\ x = 0,1,2 \end{cases}$$

then the primary winding current waveform can be obtained,as shown in Fig. 12. From (26), we know that the primary equivalent inductance determines the current ripple of primary winding. If limiting the current amplitude to I_m, the primary equivalent inductance during the shoot-through zero state can be expressed as

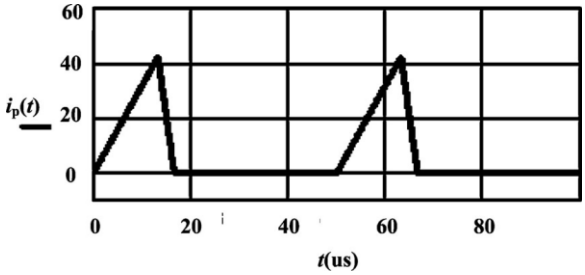

Fig. 12. Waveform of primary winding current

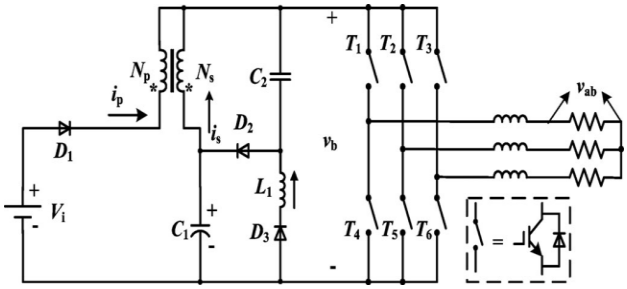

Fig.13.Simulation and prototype system of configuration

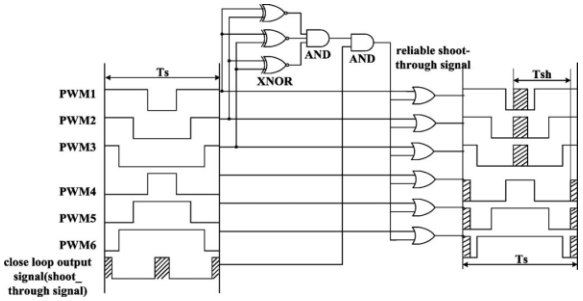

Fig. 14. Control circuit diagram for inverter switches

V. SIMULATION RESULTS

Simulation has been performed to confirm the previous analysis. Fig. 13 and 14 shows the circuit configuration with the circuit parameters as: *Vi* =330V, *Lp* = 332.3 μH, *Ls* = 1.87 mH,*k* = 0.95, *C*1 =10 μF, *C*2 = 40 μF, *L*1 = 30 μH, and *P*o= 800 VA. The system is intended to produce a three-phase 220 V ac output from a relative low level input source. Fig. 14 shows the control circuit diagram for inverter switches. Fig. 15 shows the simulation waveforms. It is clear that the bus voltage is stepped up to 700V, indicating a successful boost inverting operation of the converter. In this case, the modulation index was set to 0.86, the shoot-through duty cycle was set to 0.255, and the switching frequency was 8 kHz. The shoot-through zero state was inserted in every traditional open-zero state, achieving an equivalent switching frequency of 16 kHz viewed from the impedance network. Fig. 15(c) illustrates that the output phase voltage is constant during input voltage transient.

At load side the fig.18(d) shows the torque remains constant at rated speed .Based on the torque,speed charcterstics the torque will be droped at maxium speed.

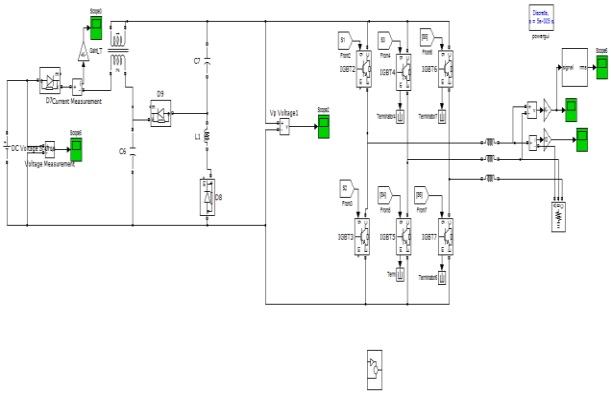

Fig. 15. Simulation diagram single stage boost inverter with coupled inductor

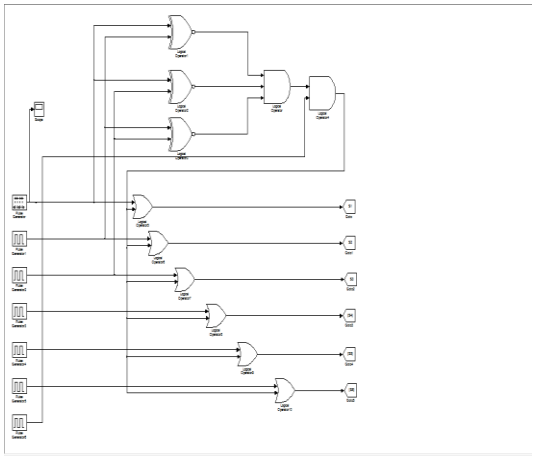

Fig. 16.simulation diagram of control circuit

$$L_{eq0\_p} = \frac{V_i \times D_0 \times T_{sh}}{I_m}$$

According to (23), the primary winding inductance *Lp* can be obtained from the relationship of primary equivalent inductance and actual primary winding inductance in one shoot-through zero state. The secondary winding inductance can also be found according to (5).

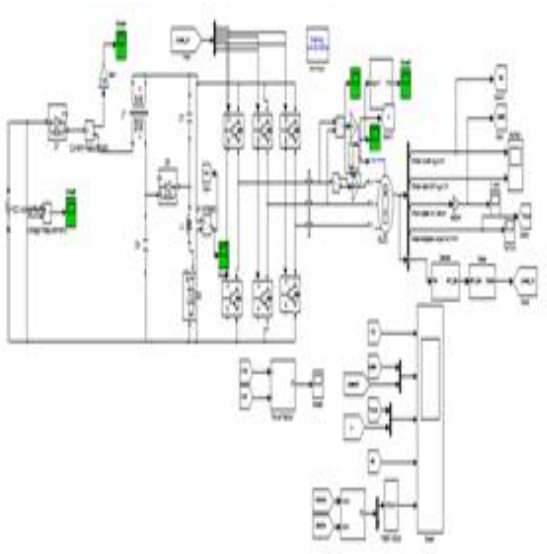

Fig.17 simulation diagram of single stage boost inverter with PMBLDC Motor

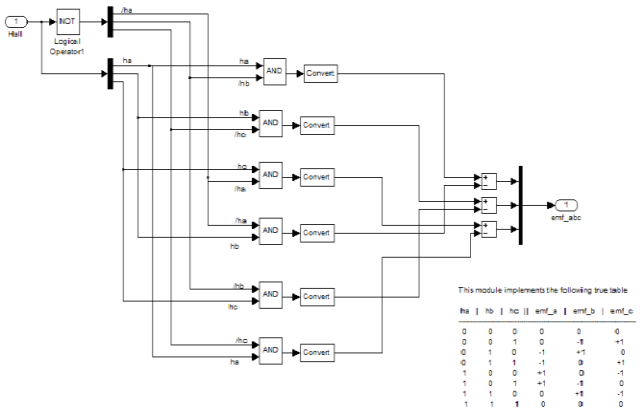

(a) Emf signals from hall sensors

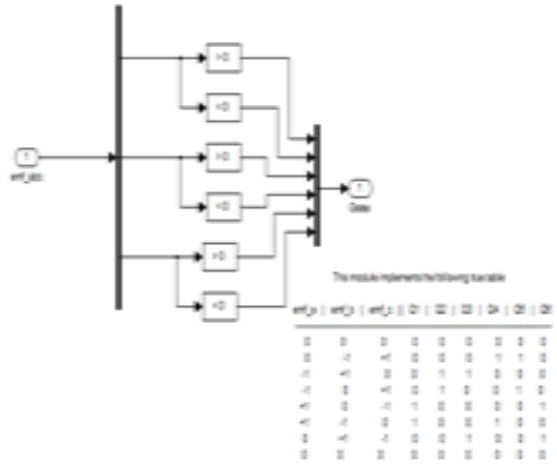

(b)switching signals from emfs

Fig (18).control circuits to feed back to the VSI

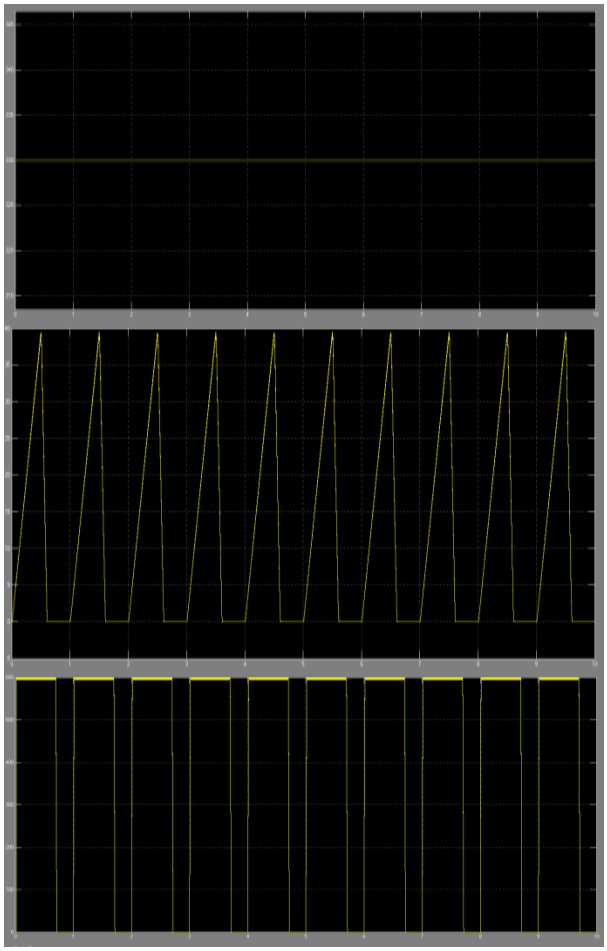

(a)Input voltage($v_{1)}$,primary winding current(i_p),bus voltage(v_b).

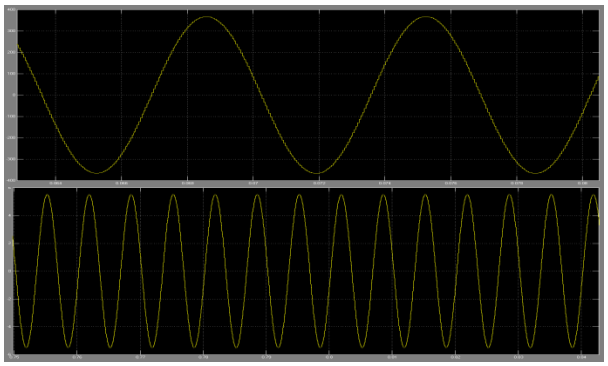

(b) Phase voltage(v_{ab}),phase current(i_a).

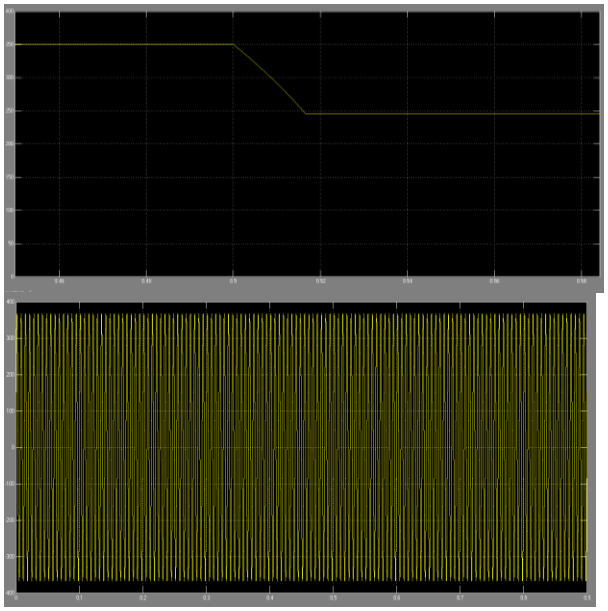

(c) Link voltage (v_1),phase voltage(v_{ab}).

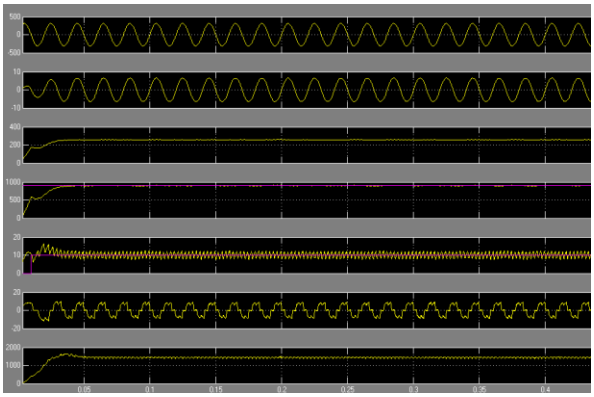

(d) Starting performance of the PMBLDCM drive at 900 rpm

Fig. 18. Simulation waveform

VI. CONCLUSION

This paper has presented a single-stage boost inverter with coupled inductor, which exhibits several merits.

1) It employs a unique impedance network including Coupled inductor to connect the three-phase inverter bridge to the power source. By designing the coupled inductor properly and adjusting the previously forbidden shoot-through zero state, the magnitude of the bus voltage can be greatly stepped up.

2) By configuring turn ratio and coupling coefficient of the coupled inductor differently, the impedance network can work in two boost modes making it suitable for different inverting applications.

3) Shoot-through states, which are forbidden in conventional VSIs, are utilized to store and transfer energy within the impedance network to boost the amplitude of the bus voltage. Waveform distortion of the ac output voltage caused by dead time is essentially avoided

4) The required voltage is obtained at load side to drive the PMBLDC Motor.

5) The PMBLDC Motor can be used for constant speed applications like blowers, pumps, fans because open loop control is used.

REFERENCES

[1] B. Bose, "Global warming: Energy, environmental pollution, and the impact of power electronics," *IEEE Trans. Ind. Electron. Mag.*, vol. 4, no. 1,pp. 6–17, Mar. 2010.

[2] Z. Chen, J. M. Guerrero, and F. Blaabjerg, "A review of the state of the art of power electronics for wind turbines," *IEEE Trans. Power Electron.*,vol. 24, no. 8, pp. 1859–1875, Aug. 2009.

[3] T. Kerekes, M. Liserre, R. Teodorescu, and C. Klumpner, "Evaluation of three-phase transformerless photovoltaic inverter topologies," *IEEE Trans. Power Electron.*, vol. 24, no. 9, pp. 2202–2211, Sep. 2009.

[4] M. Mohr, W. T. Franke, B. Wittig, and F. W. Fuchs, "Converter systems for fuel cells in the medium power range-a comparative study," *IEEE Trans. Ind. Electron.*, vol. 57, no. 6, pp. 2024–2032, Jan. 2010.

[5] B. Kroposki, C. Pink, R. Deblasio, H. Thomas, M. Simoes, and P. K. Sen,"Benefits of power electronic interfaces for distributed energy systems,"*IEEE Trans. Energy Convers.*, vol. 25, no. 3, pp. 901–908, Sep. 2010.

[6] M. Mohr, W. T. Franke, B. Wittig, and F. W. Fuchs, "Converter systems for fuel cells in the medium power range—A comparative study," *IEEE Trans. Ind. Electron.*, vol. 57, no. 6, pp. 2024–2032, Jun. 2010.

[7] R.-J. Wai, W.-H. Wang, and C.-Y. Lin, "High-performance stand-alone photovoltaic generation system," *IEEE Trans. Ind. Electron.*, vol. 55,no. 1, pp. 240–250, Jan. 2008.

[8] B. Yang, W. Li, Y. Zhao, and X. He, "Design and analysis of a gridconnected photovoltaic power system," *IEEE Trans. Power Electron.*,vol. 25, no. 4, pp. 992–1000, Apr. 2010.

[9] S.-H. Hwang and J.-M. Kim, "Dead time compensation method for voltage-fed PWMinverter," *IEEE Trans. Energy Convers.*, vol. 25, no. 1,pp. 1–10, Sep. 2010.

[10] L. Chen and F. Z. Peng, "Dead-time elimination for voltage source inverters," *IEEE Trans. Power Electron.*, vol. 23, no. 2, pp. 191–197, Mar.2008.

[11] L. H. Zhang, X. Yang, and X. F. Yao, "An isolated single stage buckboost inverter," in *Proc. IEEE Power Electron. Spec. Conf.*, 2008, pp. 2389–2395.

[12] S. H. Hosseini, S. Danyali, and A. Y. Goharrizi, "Single stage single phase series-grid connected PV system for voltage compensation and power supply," in *Proc. IEEE Power Energy Soc. Gen. Meet.*, 2009, pp. 1–7.

[13] Y. Zhaoyang, J. Li,W. Zhang, Q. Zhang, Y. Zheng, andW.Wu, "Topology family and the simulation of 'BOOK' differential single stage inverter," in *Proc. IEEE Power Electron. Distrib. Generation Syst. Conf.*, 2010,pp. 204–209.

[14] B. Sahan, A. N. Vergara, N. Henze, A. Engler, and P. Zacharias, "A singlestage PVmodule integrated converter based on a low-power current-source inverter," *IEEE Trans. Ind. Electron.*, vol. 55, no. 7, pp. 2602–2609, Jul. 2008.

[15] P. C. Loh, P. C. Tan, F. Blaabjerg, and T.K. Lee, "Topological development and operational analysis of buck-boost current source inverters for energy conversion applications," in *Proc. IEEE Power Electron. Spec. Conf.*, 2006, pp. 1–6.

[16] F. Z. Peng, "Z-source inverter," *IEEE Trans. Ind. Appl.*, vol. 39, no. 2, pp. 504–510, Mar. 2003.

[17] Y. Huang, M. Shen, F. Z. Peng, and J. Wang, "Z-source inverter for residential photovoltaic systems," *IEEE Trans. Power Electron.*, vol. 21, no. 6, pp. 1776–1782, Nov. 2006.

[18] F. Z. Peng, M. Shen, and K. Holland, "Application of Z-source inverter for traction drive of fuel cell-battery hybrid electric vehicles," *IEEE Trans. Power Electron.*, vol. 22, no. 3, pp. 1054–1061, May 2007.

[19] U. Supatti and F. Z. Peng, "Z-source inverter based wind power generation system," in *Proc. IEEE Sustainable Energy Technol. Conf.*, 2008, pp. 634–638.

[20] M. Shen and F. Z. Peng, "Operation modes and characteristics of the Zsource inverter with small inductance or low power factor," *IEEE Trans.Ind. Electron.*, vol. 55, no. 1, pp. 89–96, Jan. 2008.

[21] J. Anderson and F. Z. Peng, "Four quasi-Z-source inverters," in *Proc. IEEE Power Electron. Spec. Conf.*, 2008, pp. 2743–2749.

[22] K. Nishida, T. Ahmed, andM. Nakaoka, "A cost-effective high-efficiency
power conditioner with simple MPPT control algorithm for wind-power grid integration," *IEEE Trans. Ind. Electron.*, vol. 47, no. 2, pp. 893–900,Jun. 2011.

[23] K. Zhou and D. Wang, "Relationship between space-vector modulation and three-phase carrier-based PWM: A comprehensive analysis," *IEEE Trans. Ind. Electron.*, vol. 49, no. 1, pp. 186–196, Feb. 2002.

[24] F. Z. Peng, M. Shen, and Z. Qian, "Maximum boost control of the z-source inverter," *IEEE Trans. Power Electron.*, vol. 20, no. 4, pp. 833–838, Jul.2005.

[25] M. Shen, J. Wang, A. Joseph, and F. Z. Peng, "Constant boost control of the z-source inverter to minimize current ripple and voltage stress," *IEEE Trans. Ind. Electron.*, vol. 42, no. 3, pp. 770–778, May/Jun. 2006.

[26] G. Zhu and K. Wang, "Modeling and design considerations of coupled inductor converters," in *Proc. IEEE Appl. Power Electron. Conf.*, 2010, pp. 7–13.

[21] J. Anderson and F. Z. Peng, "Four quasi-Z-source inverters," in *Proc.IEEE Power Electron. Spec. Conf.*, 2008, pp. 2743–2749.

[22] K. Nishida, T. Ahmed, andM. Nakaoka, "A cost-effective high-efficiencybpower conditioner with simple MPPT control algorithm for wind-power grid integration," *IEEE Trans. Ind. Electron.*, vol. 47, no. 2, pp. 893–900, Jun. 2011.

[23] K. Zhou and D. Wang, "Relationship between space-vector modulation and three-phase carrier-based PWM: A comprehensive analysis," *IEEETrans. Ind. Electron.*, vol. 49, no. 1, pp. 186–196, Feb. 2002.

[24] F. Z. Peng, M. Shen, and Z. Qian, "Maximum boost control of the z-source inverter," *IEEE Trans. Power Electron.*, vol. 20, no. 4, pp. 833–838, Jul.2005.

[25] M. Shen, J. Wang, A. Joseph, and F. Z. Peng, "Constant boost control of the z-source inverter to minimize current ripple and voltage stress," *IEEE Trans. Ind. Electron.*, vol. 42, no. 3, pp. 770–778, May/Jun. 2006.

[26] G. Zhu and K. Wang, "Modeling and design considerations of coupled inductor converters," in *Proc. IEEE Appl. Power Electron. Conf.*, 2010,pp. 7–13.

[27] Yufei Zhou."Single Stage Boost Inverter With Coupled Inductor,"*IEEE Trans.Power electronics*,Vol.27,no.4,April-2012

